

# Noise2Sim – Similarity-based Self-Learning for Image Denoising

Chuang Niu Fenglei Fan Qing Lyu and Ge Wang  
 Rensselaer Polytechnic Institute  
 110 8th Street, Troy, New York 12180, USA  
 {niu, fanf2, lyuq, wangg6}@rpi.edu

## Abstract

Despite achieving the best performance in image denoising, the supervised deep denoising methods require paired noise-clean data which are often unavailable. To address this challenge, **Noise2Noise** is based on the fact that paired noise-clean images can be replaced by paired noise-noise images that are easier to collect. However, in many scenarios the collection of paired noise-noise images is still impractical. To bypass labeled images, **Noise2Void** methods predict masked pixels from their surroundings with single noisy images only but the denoising performance still needs improvements. An observation on classic denoising methods is that **non-local mean** (NLM) outcomes are typically superior to locally denoised results. On the other hand, it is pitiful that Noise2Void does not utilize self-similarities in an image as NLM methods do. Here we propose **Noise2Sim**, an NLM-inspired self-learning method for image denoising. Specifically, Noise2Sim leverages the self-similarity of image pixels to train the denoising network, requiring single noisy images only. Our theoretical analysis shows that Noise2Sim tends to be equivalent to Noise2Noise under mild conditions. To efficiently manage the computational burden for globally searching similar pixels, we design a two-step procedure to provide data for Noise2Sim training. Extensive experiments demonstrate the superiority of Noise2Sim on common benchmark datasets.

## 1. Introduction

Image denoising is to recover signals hidden in a noisy background. Since noise is a statistical fluctuation governed by quantum mechanics, denoising is generally achieved by an mean/averaging operation. For example, local averaging methods can perform Gaussian smoothing [17], anisotropic filtering [21][5], and neighborhood filtering [31][24][26]. On the other hand, non-local averaging methods rely on various non-local means with Gaussian kernel based weights [4], or via non-local collaborative filtering in the transform domain [6]. Remarkably, the non-local methods usually

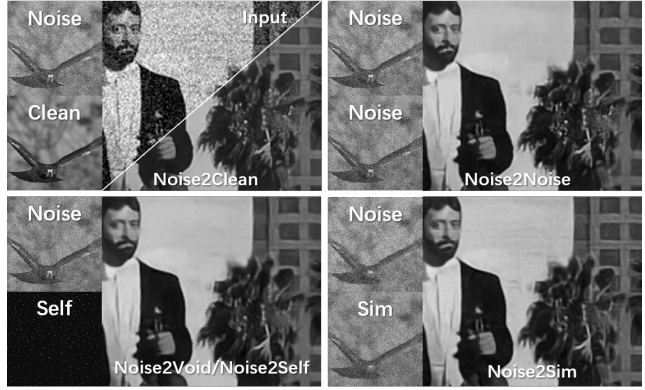


Figure 1. Comparison of different deep denoising methods. *Noise2Clean* methods require paired noise-clean samples for network training. *Noise2Noise* method takes paired noise-noise samples in the training process, which are easier to collect than Noise2Clean counterparts but still impractical in many scenarios. *Noise2Void* and *Noise2Self* methods propose to predict a small portion of excluded pixels with their local neighbors only using single noisy images during training. Beyond these methods, *Noise2Sim* leverages self-similarities in an image and constructs training images using the single noisy image itself in the same spirit of non-local means.

outperform the local methods, as images usually consist of self-similar/repeated patterns that can be leveraged in recovering signals coherently. Over recent years, the area of image denoising has been dominated by deep convolutional neural networks (CNNs). Different from the traditional methods that directly denoise an image based on an explicit model, the deep denoising methods optimize a CNN using many training images, and then use the trained model to predict the denoised image, achieving better results at less runtime than the traditional non-local methods.

Traditionally, deep denoising methods require many pairs of noise-clean images to train the networks. However, such noise-clean image pairs cannot be obtained in many practical applications. To relax the requirement of paired noise-clean samples, the Noise2Noise method [15] trains the CNN with paired noise-noise images that share

the same content but instantiated with different noises. It is shown that the Noise2Noise training tends to optimize a network up to a Noise2Clean quality under the assumption of zero-mean noises. However, the collection of paired noisy images are not practical either in many scenarios. Therefore, increasing efforts are made to develop unsupervised learning methods that train the denoising network with single noisy images. Noise2Void [12] proposed to predict the center pixel from its local neighbors, achieving promising denoising results using single noisy images only. However, it is pitiful that Noise2Void doesn't utilize self-similarities in an image as NLM methods do, while self-similarity plays a critical role in modern sciences.

Inspired by the established successes of non-local means [4] and the promising results of Noise2Noise [15], here we propose Noise2Sim to synergize these prior arts. Specifically, our Noise2Sim approach learns a CNN via self-consistent mapping between center pixels of non-local similar patches and enables a new type of unsupervised image denoising possibilities. Noise2Noise has shown that using paired noisy pixels with zero-mean noise to train a CNN will converge to what the network learns using clean pixels as the target. As paired noise-noise data are often unavailable in real applications, here we propose to approximately construct such paired noisy images only from the single noisy images. Under the assumption of non-local methods that an image usually consists of self-similarities/repeated patterns, a set of similar pixels in similar image patches can be globally searched for each pixel in a whole image. Then, a similar noisy image can be constructed by replacing each original pixel with one of the searched similar pixels. In Fig. 1, we compare the training samples used by the Noise2Clean, Noise2Noise, Noise2Void/Noise2Self methods, and our Noise2Sim method.

Theoretically, Noise2Sim tends to be equivalent to Noise2Noise if the values of similar pixels are sufficiently close and noises are independent given specific signals. Ideally, when the difference between the similar pixels is zero, the Noise2Sim result is equivalent to the Noise2Noise counterpart, as explained in Subsection 3.2. Furthermore, a training dataset for Noise2Sim is significantly larger than that for Noise2Void, with the latter being a subset of the former. That is, Noise2Sim is a non-local mean version of Noise2Void. Although it is a non-local mean method, Noise2Sim is as fast as Noise2Noise and Noise2Void in the inference stage, because it only does the non-local searching for training. Technically, to efficiently manage the computational burden of globally searching similar pixels, we design a two-step procedure to prepare training data. Also, a refined training strategy can be used for better estimation of similarity between image patches, in hope of further improved denoising results.

The main contributions of this paper are as follows:

*First*, we propose an NLM-inspired self-supervised learning method for image denoising that learns to map between similar pixels and only requires single noisy images for training. *Second*, we theoretically prove that Noise2Sim tends to be equivalent to Noise2Noise. *Third*, we technically develop a two-step procedure to efficiently manage the computational burden associated with globally searching of similar pixels in preparing data for Noise2Sim training. Also, a refined training strategy is introduced to use Noise2Sim results for further Noise2Sim denoising, which can further improve the denoising performance in some cases. *Fourth*, extensive experiments demonstrate the superiority of our Noise2Sim method on common benchmark datasets, and codes have been made publicly available at <https://github.com/niuchuangnn/noise2sim>.

## 2. Related Work

Since image denoising has been among the central problems, a large variety of denoising methods were developed over the past decades. Here we briefly review the results most relevant to our Noise2Sim method, especially traditional non-local mean (NLM) methods and deep denoising methods in different supervision modes including fully-supervised, weakly-supervised, and unsupervised or self-supervised learning. It is noted that some of these methods can be used for not only image denoising but also for image restoration (e.g., image super-resolution) and other similar tasks but here we only focus on image denoising.

### 2.1. Non-local Mean Methods

Non-local means (NLM) [4] is a classic non-local denoising approach. In contrast to the local denoising methods that use a mean value of a group of pixels surrounding a target pixel for its refinement, NLM takes a weighted mean of all pixels in an image, where the weights are determined by similarities of the image patches where these pixels are centrally located to the image patch for the target pixel. Often times, NLM reveals more details with better clarity than local denoising methods. The basic idea of non-local methods is that most images contain self-similarities/repeated patterns that can be utilized to augment data and recover signals. Based on this idea, many non-local methods were developed, such as BM3D [6], LSSC [19], NCSR [7], and WNNM [8], just to name a few. Despite their superior performance, the non-local mean methods demand longer searching time, which is a practical issue in many applications such as real-time video image processing.

### 2.2. Deep Denoising Methods

**Fully-supervised** deep denoising methods train a CNN with many paired noise-clean images that can be curated in advance. Jain *et al.* first formulated denoising as a regression task and trained a CNN by minimizing a loss function

of the prediction and clean targets [10]. In [32], a very deep CNN architecture with residual learning was introduced, effectively handling multiple levels of noise. At the same time, in [20] a very deep encoding-decoding model was designed with skip-layer connections for image restoration. In [25], a very deep persistent memory network was used with a memory block for image restoration. In the context of fluorescence microscopy, a content-aware image restoration method was introduced along with freely available software [27]. Although the supervised denoising/restoration methods were successfully applied to a variety of problems, they critically depend on paired noise-clean data which are costly to prepare or impractical to collect.

**Weakly-supervised** deep denoising method relax the requirement of paired noise-clean images to the use of paired noise-noise data or unpaired noise and clean images. The Noise2Noise method [15] uses paired noisy images to train a CNN to achieve an equivalent denoising performance under the assumption of zero-mean noise. In [29], Wu *et al.* proposed a two-step unpaired learning method for image denoising. They first leverage the self-learning methods to train a denoising model and a noising model, which are then applied on the unpaired noisy and clean images respectively to generate paired datasets. Finally, the generated image pairs are used to train the final denoising model.

**Unsupervised** deep denoising methods have recently attracted a major attention because they are least restrictive and most desirable in practice, where only single noisy images are available. Recently, Noise2Void [12] and the concurrent Noise2Self methods [2] train a network to predict masked pixels using their neighbors. Interestingly, in [13] a probabilistic Noise2Void model uses a maximum likelihood strategy to predict per-pixel intensity distributions instead of a specific pixel value only. Based on Noise2Void, Laine *et al.* redesigned the blind-spot network that takes several rotated images as the inputs and merge the corresponding outputs though a series of  $1 \times 1$  convolutions [14]. Then, assuming a known noise distribution a Bayesian reasoning strategy was proposed to optimize this blind point network. In [3], a structured Noise2Void method was presented to remove structured noise by modifying the blind mask, assuming a known noise configuration. Of particular interest, several deep denoising methods focus on training and testing on a single noisy image. The deep image prior method [16] trains a CNN to predict a noisy image of interest from a random but uniform noise, and obtain a denoised image when this process is properly terminated before convergence. Recently, Quan *et al.* suggested a Self2Self method that trains a network by mapping between random dropout images obtained with an independent Bernoulli sampling from a single noisy image [22]. In the testing stage, the trained network takes a set of independent Bernoulli sampled dropout images as the input, and averages all predictions as the out-

put. The networks of this type need to be trained for each image, and may not deliver a real-time performance.

### 3. Method

While Noise2Void and Noise2Self methods generate promising results, they miss opportunities of utilizing self-similar features in the image on which the NLM methods capitalize to outperform classic local denoising methods. Synergizing Noise2Noise and well-established NLM ideas, here we propose **Noise2Sim** as a novel self-supervised learning method, which can be trained off-line on a set of images and deployed in real-time applications.

#### 3.1. Background

To better understand Noise2Sim, we first describe its counterpart methods: Noise2Clean, Noise2Noise, and Noise2void. A noisy image  $\mathbf{x}_i$  can be decomposed into two parts, i.e.,  $\mathbf{x}_i = \mathbf{s}_i + \mathbf{n}_i$ , which is generated from the joint distribution  $p(\mathbf{s}, \mathbf{n}) = p(\mathbf{s})p(\mathbf{n}|\mathbf{s})$ , where  $\mathbf{s}_i$  and  $\mathbf{n}_i$  are the clean signal and noise respectively, and  $p$  denotes the distribution. The deep desnoising methods aim to learn a network function to recover the clean signal  $\mathbf{s}_i$  from the noisy image  $\mathbf{x}_i$ , i.e.,  $\mathbf{y}_i = f(\mathbf{x}_i; \boldsymbol{\theta})$ , where  $f$  denotes the network function with the vector of parameters  $\boldsymbol{\theta}$  to be optimized.

For Noise2Clean, each noisy image  $\mathbf{x}_i$  requires a corresponding clean image  $\mathbf{s}_i$  as the target. The parameters  $\boldsymbol{\theta}_c$  of the denoising network are optimized as

$$\boldsymbol{\theta}_c = \arg \min_{\boldsymbol{\theta}} \frac{1}{N_c} \sum_{i=1}^{N_c} \|f(\mathbf{s}_i + \mathbf{n}_i; \boldsymbol{\theta}) - \mathbf{s}_i\|_2^2, \quad (1)$$

where  $N_c$  is the number of images, and the mean squared error (MSE) loss function is adopted as in [15, 12].

For Noise2Noise, paired noisy images, i.e.,  $\mathbf{x}_i = \mathbf{s}_i + \mathbf{n}_i$  and  $\mathbf{x}'_i = \mathbf{s}_i + \mathbf{n}'_i$ , are required to train the network, where  $\mathbf{n}_i$  and  $\mathbf{n}'_i$  are two independent and zero-mean noise realizations. The parameters  $\boldsymbol{\theta}_n$  of the denoising network are optimized as

$$\boldsymbol{\theta}_n = \arg \min_{\boldsymbol{\theta}} \frac{1}{N_n} \sum_{i=1}^{N_n} \|f(\mathbf{s}_i + \mathbf{n}_i; \boldsymbol{\theta}) - (\mathbf{s}_i + \mathbf{n}'_i)\|_2^2, \quad (2)$$

where  $N_n$  is the number of paired images for Noise2Noise. Theoretically, if the conditional expectation  $\mathbb{E}[\mathbf{n}'_i | \mathbf{s}_i + \mathbf{n}_i] = 0$  is satisfied, the learned parameters  $\boldsymbol{\theta}_n$  with paired noise-noise images will be equal to  $\boldsymbol{\theta}_c$  optimized under paired noise-clean images as  $N_n \rightarrow \infty$  [28]; please refer to the supplementary material for details. As  $\mathbf{n}'_i$  is independent to  $\mathbf{n}_i$ ,  $\mathbb{E}[\mathbf{n}'_i | \mathbf{s}_i + \mathbf{n}_i] = \mathbb{E}[\mathbf{n}'_i | \mathbf{s}_i] = 0$  is true under the zero-mean noise assumption.

For Noise2Void, only noisy images are required for network training. It splits the noisy image  $\mathbf{x}_i$  into two parts, i.e.,  $\mathbf{x}_i = \mathbf{x}_i^c \cup \mathbf{x}_i^r$ . As shown in Fig. 1,  $\mathbf{x}_i^c$  contains a small set of pixels from  $\mathbf{x}_i$  and used as the targets of the rest pixels  $\mathbf{x}_i^r$ . Thus, the parameters  $\theta_v$  of the denoising network are optimized as follows:

$$\theta_v = \arg \min_{\theta} \sum_{i=1}^{N_v} \|f(\mathbf{x}_i^r; \theta) - \mathbf{x}_i^c\|_2^2, \quad (3)$$

Three assumptions are required to make the Noise2Void mapping work [12]. First, the signal value is predictable from its local surrounding noisy pixels in the receptive field of the neural network. Second, the noise components of different pixels are independent of each other. Third, the expectation of the noise component is zero, ensuring that the predicted values converge to the clean signal.

### 3.2. Noise2Sim

Here we present Noise2Sim as a new self-supervised learning method to learn a denoising neural network requiring single noisy images only. As paired noise-clean or noise-noise data are unavailable, Noise2Sim first constructs paired similar images, denoted by  $\mathbf{x}_i = \mathbf{s}_i + \mathbf{n}_i$  and  $\hat{\mathbf{x}}_i = \mathbf{s}_i + \delta_i + \mathbf{n}'_i$ , where  $\delta_i$  is the difference between the clean signal components of paired similar images, and  $\mathbf{n}_i$  and  $\mathbf{n}'_i$  are two independent and zero-mean noise realizations. Then, the network parameters  $\theta_s$  in Noise2Sim are computed in the following optimization process:

$$\theta_s = \arg \min_{\theta} \frac{1}{N_s} \sum_{i=1}^{N_s} \|f(\mathbf{s}_i + \mathbf{n}_i; \theta) - (\mathbf{s}_i + \delta_i + \mathbf{n}'_i)\|_2^2, \quad (4)$$

where  $N_s$  denotes the number of noisy similar image pairs. We have obtained the following theorem to demonstrate the effectiveness of Noise2Sim, whose proof is in the supplementary material.

**Theorem 1.** *If conditional expectation  $\mathbb{E}[\mathbf{n}'_i | \mathbf{s}_i + \mathbf{n}_i] = \mathbf{0}$ , and  $\mathbb{E}[\delta_i | \mathbf{s}_i + \mathbf{n}_i] = \mathbf{0}, \forall \theta$  and  $i$ , then  $\lim_{N_s \rightarrow \infty} \theta_s = \lim_{N_n \rightarrow \infty} \theta_n = \theta_c$ .*

**Remark:** The assumption of Noise2Sim is that the noise components of different pixels are independent to each other and have a zero mean so that  $\mathbb{E}[\mathbf{n}'_i | \mathbf{s}_i + \mathbf{n}_i] = \mathbb{E}[\mathbf{n}'_i | \mathbf{s}_i] = \mathbf{0}$ . In practice, although  $\mathbb{E}[\delta_i | \mathbf{x}_i + \mathbf{n}_i] = \mathbf{0}$  cannot be totally ensured, it is a realistic approximation due to the similarity among pixels, as empirically demonstrated in Subsection 4.3.1. Thus, Noise2Sim can be regarded as an excellent surrogate of Noise2Noise. When  $N_s \rightarrow \infty$ , Noise2Sim is functionally equivalent to Noise2Noise and Noise2Clean. In terms of the training samples, i.e.,  $\mathbf{x}_i^c \subset \mathbf{x}_i$  and  $\mathbf{x}_i^r \subset \hat{\mathbf{x}}_i$ , Noise2Sim can be regarded as a non-local

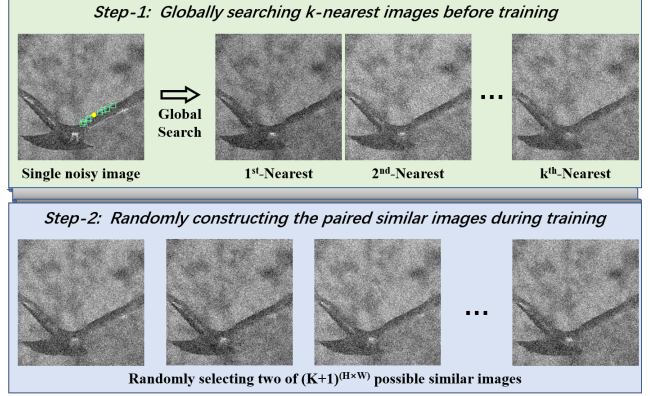


Figure 2. Process of generating data for Noise2Sim training. Step 1 is to find a set of  $k$  similar pixels for each reference pixel in a single noisy image, and form  $k$  nearest images. In the exemplary noisy image, the yellow point denotes the reference pixel, and the green boxes present its  $k$ -nearest patches whose central pixels are defined as similar pixels.  $k^{th}$  nearest subfigure indicates replacing every pixel in the original noisy image by its corresponding the  $k^{th}$  nearest pixel. Step 2 is to randomly and independently construct paired images in a pixel-wise way from the  $(k+1)$  similar images obtained in Step 1.

version of Noise2Void, leveraging both local and global information. Therefore, Noise2Sim enjoys theoretical superiority to Noise2Void.

### 3.3. Noise2Sim training

Although Noise2Sim is statistically sound under the Theorem 1, how to efficiently construct training samples is not trivial. Next, we describe the construction process of similar image pairs from a single noisy image in pixel-wise. Specifically, for each pixel  $\mathbf{x}_i(u, v)$  with the coordinate  $(u, v)$  in a given noisy image, we search for its  $k$  nearest pixels over the whole image. The distance between two pixels  $\mathbf{x}(u_1, v_1)$  and  $\mathbf{x}(u_2, v_2)$  is computed as the Euclidean distance between their surrounding patches, i.e.,  $\|\mathbf{S}(u_1, v_1) - \mathbf{S}(u_2, v_2)\|_2$ , where  $\mathbf{S}(u, v)$  denotes a square patch of an appropriate size and centered at the pixel  $\mathbf{x}(u, v)$ . Thus, each position in the image has a set of  $k+1$  similar pixels (+1 means the reference pixel included), denoted as  $\mathcal{N}(u, v) = \{\mathbf{x}(u, v), \mathbf{x}^1(u, v), \dots, \mathbf{x}^k(u, v)\}$ , where  $\mathbf{x}^j(u, v)$  denotes the  $j$ -th nearest pixel to  $\mathbf{x}(u, v)$ . As shown on the top-left image in Fig. 2, the yellow dot denotes a reference pixel, and the green boxes are the surrounding patches of searched similar pixels. Based on the searched similar pixel sets, a similar noisy image can be easily constructed by replacing every original pixel  $\mathbf{x}(u, v)$  with its similar one that is randomly selected from  $\mathcal{N}(u, v)$ . Then, a paired similar images are obtained by independently repeat the above process twice in each iteration.

It is well known that globally searching for similar pixels has a large computational cost. Clearly, the number of all



possible similar images to each given image is  $(k+1)^{H \times W}$ , where  $H$  and  $W$  represent the image size. If all similar images are prepared before training or searched on-the-fly during training, the memory space or computational time will be unacceptable. Naturally, we propose to divide the Noise2Sim training process into two steps. First, we generate  $k$ -nearest similar images from a single noisy image, which is a preprocessing step. The  $k$ -nearest similar images are obtained by sorting the  $k$ -nearest similar pixels for each and every pixel location, i.e., the  $j$ -th nearest image is  $[x^j(u, v)]_{H \times W}$ , as shown in Fig. 2. Second, given the  $k+1$  similar images, we randomly and independently construct a pair of similar images in pixel-wise on-the-fly during training. The two-step training strategy allows a real-time construction of paired similar images at little cost, and the searching time of these similar images for the first step is also acceptable using an advanced searching algorithm implemented on GPU. Certainly, there are alternative ways to select the training pairs, see our comparative study in Subsection 4.3.2. After training, the network takes the original noisy image and produces an denoised image. Since noises may harm the estimation of signal similarities, we propose to use the denoised image to further compute the similarity between signals and conduct Noise2Sim training again, which can be iteratively conducted if necessary.

## 4. Experiments

### 4.1. Implementation Details

For a fair comparison, the two-layer UNet [23] with the batch normalization [9] and residual learning was used through all our experiments, which is exactly the same as the network used for Noise2Void. Although the denoising performance can be improved with more advanced architectures, here we focus on demonstrating the feasibility and power of our novel NLM-inspired self-learning method for unsupervised denoising, instead of optimizing any particular architecture. For fast computation of searching similar pixels, we used a publicly available library<sup>1</sup>, which is powered by GPU. In the training stage, we used the same augmentation strategy as that used for Noise2Void, including random cropping followed by random 90°-rotation and mirroring. The Adam [11] algorithm with the cosine learning rate schedule [18] was deployed for training, with the initial learning rate 0.0005. Our method was implemented on the PyTorch<sup>2</sup> deep learning platform.

### 4.2. Datasets

We evaluated our proposed Noise2Sim and competitive methods on both simulated and real datasets, including commonly used BSD68 and BSD400 [32] that

consist of gray-scale images, BSD500 [1] and Kodak<sup>3</sup> containing color images, and the fluorescence microscopy datasets Fluo-C2DL-MS (MSC) and Fluo-N2DH-GOWT1 (GOWT1) only containing noisy images from the Cell Tracking Challenge. We also constructed a set of piece-wise constant phantom images added with Gaussian noises for assessing the denoising performance of Noise2Sim under the ideal condition and added with structured noises for evaluating the possibility of extending Noise2Sim to process the structured noises (see the supplementary material for details). We used the peak signal-to-noise ratio (PSNR) and the structured similarity (SSIM) index to quantify the denoising performance.

### 4.3. Empirical analysis

We evaluated alternative methods of pairing similar pixels for training the network, analyzed the hyperparameters that affect the selection of similar pixels, and tested the effectiveness of the iterative training strategy. For these purposes, we used the BSD400 dataset consisting of 400  $180 \times 180$  gray images for training, and the BSD68 dataset containing 68 gray images for testing. Gaussian noise with zero mean and different standard deviations were added.

#### 4.3.1 Estimation of $\mathbb{E}[\delta_i | s_i + n_i]$

Here we aim to empirically estimate the values of the conditional expectation  $\mathbb{E}[\delta_i | s_i + n_i]$  on the BSD400 dataset, where the standard deviation of Gaussian noise was 25. Specifically, it was estimated with the following equation

$$\hat{\mathbb{E}}[\delta_i | s_i + n_i] = \frac{1}{M} \sum_{i=1}^M (\hat{x}'_i - \hat{x}''_i), \quad (5)$$

where  $\hat{x}'_i$  and  $\hat{x}''_i$  are similar image pairs that are randomly constructed given one of BSD400 images, and  $M$  was set to  $5000 \times 400 = 2 \times 10^6$  (it means each image was repeatedly used 5000 times) that is consistent with the training process. In our experiments, we found that the values of this estimation are closed to zeros, i.e.,  $\hat{\mathbb{E}}[\delta_i | s_i + n_i] \in [-0.0014, 0.0013]$ , where  $s_i$  was normalized into  $[0, 1]$ . Thus, Noise2Sim can be regarded as a practically reasonable approximation of Noise2Noise when only single noisy images are available.

#### 4.3.2 Pairing Methods

Table 1. Results with different methods for pairing similar pixels in patches of  $3 \times 3$  for  $k = 8$  and Gaussian noise Std 25.

Pairing Method	1	2	3	4
PSNR	27.12	27.78	27.48	<b>28.15</b>

<sup>1</sup><https://github.com/facebookresearch/faiss>

<sup>2</sup><https://pytorch.org/>

<sup>3</sup><http://r0k.us/graphics/kodak/>

Given a set of  $k + 1$  similar images as described in Subsection 3.3, there are four reasonable methods for pairing them: 1) Pair the original noisy image as the input to its randomly constructed similar image as the target; 2) reverse the input and label used in 1); 3) pair the two of  $k$  sorted similar images without pixel-wise randomization; and 4) pair similar images that were randomly and independently constructed in a pixel-wise. The results in Table 1 demonstrate that the fourth pairing method achieves the best denoising performance. This is because the fourth pairing method can significantly increase the number of possible similar image pairs, i.e.,  $(k + 1)^{2HW}$ , leading to a better estimation. More analysis can be found in the supplementary material.

### 4.3.3 Hyper-parameters

Table 2. Effects on PSNR of image patch sizes vs. Gaussian noise levels.

S \ Std	5	15	25	35	45	55	65	75
$3 \times 3$	33.85	29.90	<b>28.14</b>	<b>26.73</b>	<b>25.73</b>	24.89	24.06	23.45
$5 \times 5$	<b>34.32</b>	<b>29.98</b>	28.02	26.72	25.69	24.93	24.03	23.45
$7 \times 7$	33.13	29.87	27.93	26.70	25.67	24.83	24.02	<b>23.74</b>
$11 \times 11$	32.10	29.82	27.43	26.56	25.69	24.86	<b>24.25</b>	23.71
$15 \times 15$	31.97	28.96	27.58	26.53	25.67	<b>24.94</b>	24.18	23.68

In the proposed Noise2Sim method, searching for an appropriate set of similar pixels for each reference pixel is a core task. In the search process, a size-fixed square patch window is translated over a noisy image of interest to find similar pixels. Hence, the patch size, denoted by  $S$ , is a key parameter that affects the accuracy of similarity measurement. The effect of different patch sizes vs. different Gaussian noise levels on PSNR are shown in Table 2. It can be seen in general that the denoising performance of smaller patch sizes is better for lower noise levels but that of larger patch sizes is better for higher noise levels. This is due to the fact that it requires more contextual information to estimate the similarity accurately when pixels are heavily corrupted by noise.

Table 3. Effects on PSNR of different numbers of similar pixels vs. different patch sizes for  $k = 8$  and Gaussian noise  $Std = 25$ .

S \ k	2	4	8	16	32	64
$3 \times 3$	26.93	27.90	<b>28.15</b>	28.08	27.95	27.01
$5 \times 5$	26.95	27.84	<b>28.02</b>	26.24	26.55	25.94
$7 \times 7$	26.91	27.68	<b>27.93</b>	27.71	27.50	27.28
$11 \times 11$	26.81	<b>27.58</b>	27.43	27.23	25.21	25.02
$15 \times 15$	26.78	27.15	<b>27.58</b>	26.57	26.47	24.76

Moreover, the number of selected similar pixels  $k$  determines the error term  $\delta$  defined in Subsection 3.2. Then, we evaluated the effects of different numbers of selected similar pixels on the denoising performance as shown in Table

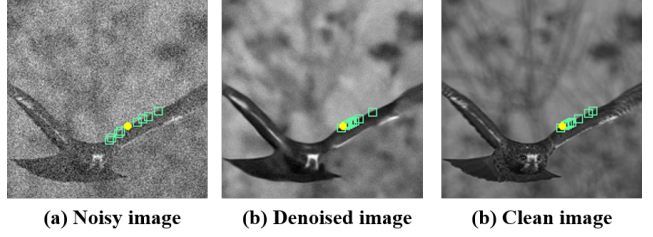


Figure 3. Distribution of similar patches in (a) an original noisy image, (b) the denoised image, and (c) the clean image.

3. The results show that the best denoising performance was generally associated with  $k = 8$  in our comparative study. These results are attributed to the fact that there is a trade-off between the error term and the number of training samples. Specifically, increasing the number of similar pixels will increase  $\delta$  values, while decreasing this number will decrease the amount of information on self-similarity. It seems that a decent balance is  $k = 8$  in our experiments.

### 4.3.4 Iterative Training

Table 4. Results of Noise2Sim with and without iterative training with respect to different Gaussian levels.

Std	5	15	25	35	45	55	65
<i>W/O</i>	33.85	29.90	28.14	26.73	25.73	24.89	24.06
<i>With</i>	34.15	30.25	28.27	26.98	25.75	24.88	24.02
<i>Upper</i>	34.22	30.54	28.60	27.14	26.08	25.15	24.33

Any estimate of similarity between image patches is necessarily compromised in a noisy image, such an estimate may be improved in a denoised image produced by a trained denoising model. That is, the Noise2Sim idea can be repeatedly applied to refine the resultant denoising model iteratively. By doing so, the similarity measures will be likely improved, leading to a superior denoising performance. Fig. 3 shows the change in the distribution of similar image patches after one iteration, and the distribution in the denoised image is very close to that in the clean image. We also computed the upper limit for the iterative training by computing the similarity measures using the clean image. Table 4 shows that the iterative training enhances the denoising performance, especially when noise level is small. When the images are severely corrupted, the initial denoising results are not good enough, even leading to a worse estimation of similar pixels.

## 4.4. Comparative Denoising Results

In this Subsection, we compared Noise2Sim with the Noise2Clean, Noise2Noise, Noise2Void, and NLM methods on the same datasets and using the same network architecture. The mean PSNR and SSIM results on whole

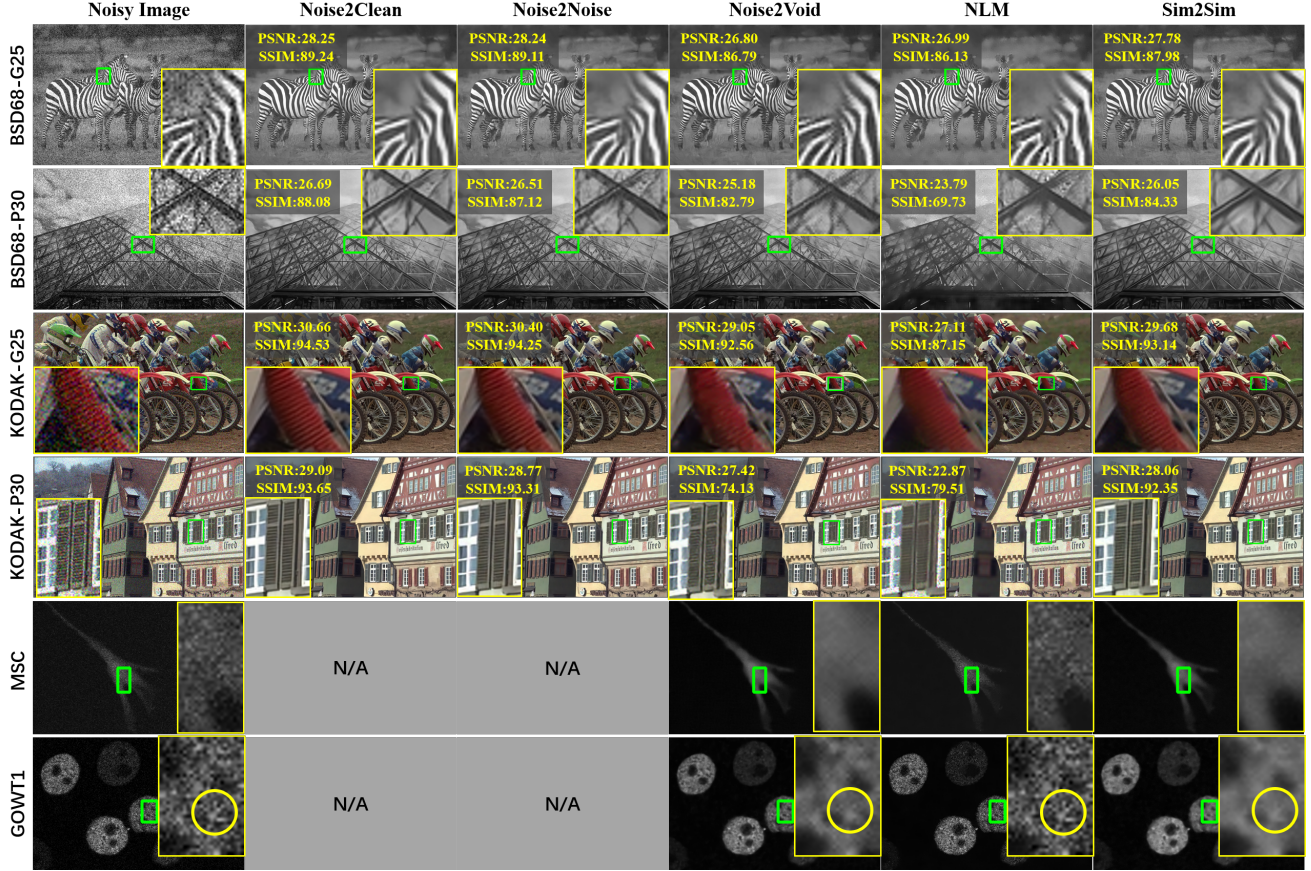


Figure 4. Visual comparison of denoising results on different datasets, where *G25* means Gaussian noise with  $Std = 25$ , and *P30* means Poisson noise with  $\lambda = 30$ . For the images with the ground truth, their PSNR and SSIM values are included. The GOWT1 and MSC datasets only contain noisy images so that the results of *Noise2Clean* and *Noise2Noise* are not available. The yellow boxes show the zoom-in regions, and the yellow circles in the last row emphasize a specific structure for visual inspection.

Table 5. Comparison of denoising results using different methods on different datasets. Here both PSNR/SSIM(%) were reported.

Dataset	N2C	N2N	N2V	NLM	Noise2Sim
BSD68-G25	28.96/89.78	28.88/89.44	27.72/86.65	27.58/85.27	28.27/88.17
BSD68-P30	28.08/88.26	27.98/87.78	27.08/85.24	24.65/77.54	27.37/85.70
Koak-G25	32.45/94.23	31.68/93.75	31.02/92.48	29.38/88.44	31.18/92.52
Koak-P30	31.74/93.65	31.52/93.41	30.35/91.34	25.99/81.05	30.44/91.56

datasets are reported in Table 5, which indicates that Noise2Sim is better than the NLM and Noise2Void methods in terms of both evaluation metrics. The visual results are shown in Fig. 4, where each row presents the results of different methods for a specific image. These results show that the proposed Noise2Sim method can effectively remove additive Gaussian noises and conditional Poisson noises in grayscale and color images. In consistent with the numerical results in Table 5, the visual results show that Noise2Sim is consistently better than the NLM and Noise2Void counterparts in general settings. The PSNR and SSIM values of individual images also support these findings.

As introduced before, the supervised learning methods Noise2Clean and Noise2Noise can do nothing for denoising some real application images, while Noise2Sim still works well. As the images in MSC and GOWT1 do not have the corresponding ground truth or co-registered independent noisy duplicate, the Noise2Clean and Noise2Noise methods cannot be applied. In [12], the authors pointed out a limitation of the Noise2Void method that it cannot preserve grainy features when the local predictability is in question. Consistent to the known limitation, some grainy structures are missed in our verified Noise2Void images, with some black "holes" presented, as shown in the zoom-in regions of the last two rows in Fig. 4. In contrast, our Noise2Sim images well preserve structural subtleties, as information on self-similarities is fully utilized in our training stages.

Moreover, we also evaluated different methods for denoising different levels of noises as shown in Table 6. When the noise level is very small, i.e.,  $std = 5$ , NLM performs better than both Noise2Void and Noise2Sim. In contrast, Noise2Void is superior for denoising the images that



Table 6. Result using different denoising methods on the datasets corrupted by Gaussian noise at different levels.

Std	5	15	25	35	45	55	65	75
<i>N2C</i>	37.89	31.62	28.96	27.33	26.17	25.33	24.58	24.05
<i>N2N</i>	37.84	31.39	28.88	27.22	26.01	25.28	24.42	23.96
<i>N2V</i>	31.81	29.26	27.72	26.61	25.36	24.84	23.95	23.50
<i>NLM</i>	35.31	29.92	27.58	26.07	24.95	24.06	23.29	22.63
<i>N2S</i>	34.15	30.25	28.27	26.98	25.75	24.89	24.06	23.45

are severely corrupted ( $std = 75$ ). With increasing the noise level, the accuracy of searching similar pixels will be comprised so that the denoising performance of Noise2Sim training will be degraded. Although Noise2Sim cannot consistently surpass the NLM and Noise2Void counterparts especially under the extreme conditions, Noise2Sim is obviously better for a large range of noise level  $15 \leq std \leq 65$ . These results further demonstrate the superiority of Noise2Sim.

#### 4.5. Results of Processing A Single Noisy Image

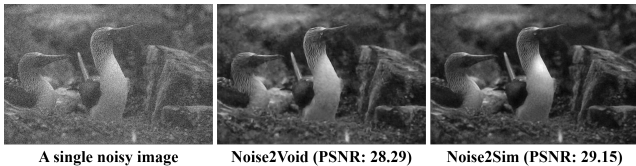


Figure 5. Results of denoising a single noisy image.

Although we mainly focus on the dataset based training paradigm, the proposed Noise2Sim can also process a single noisy image that training and testing are performed on the same single image. The results of processing the single image are shown in Figure 5, we can see that Noise2Sim also outperforms Noise2Void in this setting. Obviously, the local information in a single image used for training Noise2Void is limited, while the non-local similarity-based counterpart is effectively leveraged for Noise2Sim.

#### 4.6. Results on Simulated Ideal Dataset

Here we evaluated the denoising performance of the Noise2Sim method under the ideal condition that  $\delta = 0$ ,

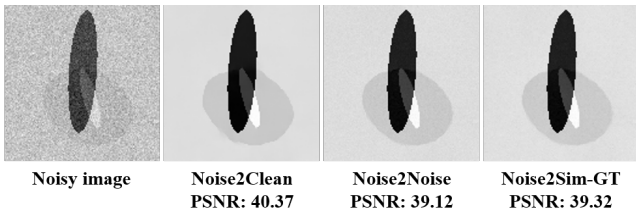


Figure 6. Result obtained using different denoising methods on the simulated dataset, with the PSNR values on the test dataset.

which is denoted as *Noise2Sim-GT*. To satisfy this condition, we construed a set of piece-wise constant phantom images corrupted by Gaussian noise with *Std* 25. When constructing the training samples for *Noise2Sim-GT*, we assumed the known masks over the piece-wise regions, and thus  $k$  pixels in the same region of the reference pixel were randomly selected as its  $k$ -nearest similar pixels. The rest steps remained the same as those described in Subsection 3.3. The results using different denoising methods on the simulated dataset are in Fig. 6, demonstrating the Noise2Sim-GT method is indeed equivalent to the Noise2Noise method and being consistent to the analysis in Subsection 3.2.

### 5. Discussions

The conditional independence assumption does not support the use of Noise2Sim in suppressing structural noise, which is also the limitation of Noise2Void. Recently, an variant of Noise2Void, Structured Noise2Void [3], was proposed to remove horizontally or vertically correlated noise. Along this direction, we can extend Noise2Sim for more types of noises including structured noises. Specifically, with piece-wise constant or piece-wise polynomial [30] segmentation masks, similar patches can be found in semantically similar regions and paired to generate data for network training. Also, pixel-level mappings can be generalized to patch-level mappings so that coherent noises can be suppressed. Experimental results on the feasibility to remove structural noises can be found in the supplementary.

It is underlined that in this initial study the Euclidean distance is used to measure the similarity between patches. More advanced measures can be used for further improvements. Self-similarity exhibits itself in many ways: direct as measured by the Euclidean distance, indirect through scaling, reflection, and rotation, or even hidden in a transform domain. Hence, Noise2Sim can be further developed for an optimized performance in a task-specific fashion.

### 6. Conclusion

We have presented a novel similarity-based self-learning approach for image denoising that only requires single noisy images to train the CNN. Theoretically, we have compared the Noise2Clean, Noise2Noise, and Noise2Sim methods, and shown that they tend to be equivalent under mild practical conditions. Technically, a two-step learning scheme has been designed for efficient training data generation. Experimentally, our results have systematically demonstrated the feasibility and superiority of Noise2Sim on both simulated and real datasets. Furthermore, our Noise2Sim approach can be extended from multiple views, such as using finer similarity measures between pixels/patches, extracting more self-similarity information,



incorporating the Bayesian reasoning, and removing correlated noises in diverse applications.

## References

- [1] Pablo Arbelaez, Michael Maire, Charless Fowlkes, and Jitendra Malik. Contour detection and hierarchical image segmentation. *IEEE Trans. Pattern Anal. Mach. Intell.*, 33(5):898–916, May 2011.
- [2] Joshua Batson and Loic Royer. Noise2Self: Blind denoising by self-supervision. volume 97 of *Proceedings of Machine Learning Research*, pages 524–533. PMLR, 09–15 Jun 2019.
- [3] C. Broaddus, A. Krull, M. Weigert, U. Schmidt, and G. Myers. Removing structured noise with self-supervised blind-spot networks. In *2020 IEEE 17th International Symposium on Biomedical Imaging (ISBI)*, pages 159–163, 2020.
- [4] A. Buades, B. Coll, and J. . Morel. A non-local algorithm for image denoising. In *2005 IEEE Computer Society Conference on Computer Vision and Pattern Recognition (CVPR’05)*, volume 2, pages 60–65 vol. 2, 2005.
- [5] Francine Catté, Pierre-Louis Lions, Jean-Michel Morel, and TOMEU COLL. Image selective smoothing and edge detection by nonlinear diffusion. *SIAM Journal on Numerical Analysis*, 29(1):182–193, 1992.
- [6] K. Dabov, A. Foi, V. Katkovnik, and K. Egiazarian. Image denoising by sparse 3-d transform-domain collaborative filtering. *IEEE Transactions on Image Processing*, 16(8):2080–2095, 2007.
- [7] W. Dong, L. Zhang, G. Shi, and X. Li. Nonlocally centralized sparse representation for image restoration. *IEEE Transactions on Image Processing*, 22(4):1620–1630, 2013.
- [8] S. Gu, L. Zhang, W. Zuo, and X. Feng. Weighted nuclear norm minimization with application to image denoising. In *2014 IEEE Conference on Computer Vision and Pattern Recognition*, pages 2862–2869, 2014.
- [9] Sergey Ioffe and Christian Szegedy. Batch normalization: Accelerating deep network training by reducing internal covariate shift. volume 37 of *Proceedings of Machine Learning Research*, pages 448–456, Lille, France, 07–09 Jul 2015. PMLR.
- [10] Viren Jain and Sebastian Seung. Natural image denoising with convolutional networks. In D. Koller, D. Schuurmans, Y. Bengio, and L. Bottou, editors, *Advances in Neural Information Processing Systems 21*, pages 769–776. 2009.
- [11] Diederik P. Kingma and Jimmy Ba. Adam: A method for stochastic optimization. In Yoshua Bengio and Yann LeCun, editors, *ICLR*, 2015.
- [12] A. Krull, T. Buchholz, and F. Jug. Noise2void - learning denoising from single noisy images. In *2019 IEEE/CVF Conference on Computer Vision and Pattern Recognition (CVPR)*, pages 2124–2132, 2019.
- [13] Alexander Krull, Tomáš Vičar, Mangal Prakash, Manan Lalit, and Florian Jug. Probabilistic noise2void: Unsupervised content-aware denoising. *Frontiers in Computer Science*, 2:5, 2020.
- [14] Samuli Laine, Tero Karras, Jaakko Lehtinen, and Timo Aila. High-quality self-supervised deep image denoising. In H. Wallach, H. Larochelle, A. Beygelzimer, F. d’Alché-Buc, E. Fox, and R. Garnett, editors, *Advances in Neural Information Processing Systems 32*, pages 6970–6980. 2019.
- [15] Jaakko Lehtinen, Jacob Munkberg, Jon Hasselgren, Samuli Laine, Tero Karras, Miika Aittala, and Timo Aila. Noise2Noise: Learning image restoration without clean data. volume 80, pages 2965–2974, 10–15 Jul 2018.
- [16] V. Lempitsky, A. Vedaldi, and D. Ulyanov. Deep image prior. In *2018 IEEE/CVF Conference on Computer Vision and Pattern Recognition*, pages 9446–9454, 2018.
- [17] M Lindenbaum, M Fischer, and A Bruckstein. On gabor’s contribution to image enhancement. *Pattern Recognition*, 27(1):1 – 8, 1994.
- [18] I. Loshchilov and F. Hutter. Sgdr: Stochastic gradient descent with warm restarts. In *ICLR*, 2017.
- [19] J. Mairal, F. Bach, J. Ponce, G. Sapiro, and A. Zisserman. Non-local sparse models for image restoration. In *2009 IEEE 12th International Conference on Computer Vision*, pages 2272–2279, 2009.
- [20] Xiaojiao Mao, Chunhua Shen, and Yu-Bin Yang. Image restoration using very deep convolutional encoder-decoder networks with symmetric skip connections. In D. D. Lee, M. Sugiyama, U. V. Luxburg, I. Guyon, and R. Garnett, editors, *Advances in Neural Information Processing Systems 29*, pages 2802–2810. 2016.
- [21] P. Perona and J. Malik. Scale-space and edge detection using anisotropic diffusion. *IEEE Transactions on Pattern Analysis and Machine Intelligence*, 12(7):629–639, 1990.
- [22] Yuhui Quan, Mingqin Chen, Tongyao Pang, and Hui Ji. Self2self with dropout: Learning self-supervised denoising from single image. In *Proceedings of the IEEE/CVF Conference on Computer Vision and Pattern Recognition (CVPR)*, June 2020.
- [23] Olaf Ronneberger, Philipp Fischer, and Thomas Brox. U-net: Convolutional networks for biomedical image segmentation. In Nassir Navab, Joachim Hornegger, William M. Wells, and Alejandro F. Frangi, editors, *MICCAI*, pages 234–241, 2015.
- [24] S M Smith and J M Brady. SUSAN-A New Approach to Low Level Image Processing. *Int. Journal of Computer Vision*, 23(1):45–78, 1997.
- [25] Ying Tai, Jian Yang, Xiaoming Liu, and Chunyan Xu. Memnet: A persistent memory network for image restoration. In *Proceedings of the IEEE International Conference on Computer Vision (ICCV)*, Oct 2017.
- [26] C. Tomasi and R. Manduchi. Bilateral filtering for gray and color images. In *Sixth International Conference on Computer Vision (IEEE Cat. No.98CH36271)*, pages 839–846, 1998.
- [27] Martin Weigert, Uwe Schmidt, Tobias Boothe, Andreas Müller, Alexandr Dibrov, Akanksha Jain, Benjamin Wilhelm, Deborah Schmidt, Coleman Broaddus, Siân Culley, Mauricio Rocha-Martins, Fabián Segovia-Miranda, Caren Norden, Ricardo Henriques, Marino Zerial, Michele Solimena, Jochen Rink, Pavel Tomancak, Loic Royer, Florian Jug, and Eugene W. Myers. Content-aware image restoration: Pushing the limits of fluorescence microscopy. *Nature Methods*, 15(12):1090–1097, 2018.

- [28] D. Wu, K. Gong, K. Kim, X. Li, and Q. Li. Consensus neural network for medical imaging denoising with only noisy training samples. In *MICCAI 2019*, 2019.
- [29] Xiaohe Wu, Ming Liu, Yue Cao, Dongwei Ren, and Wangmeng Zuo. Unpaired learning of deep image denoising. In *European Conference on Computer Vision (ECCV)*, 2020.
- [30] Jiansheng Yang, Hengyong Yu, and Ge Wang. High order total variation minimization for interior tomography. *Inverse Probl.*, 26(3):350131–3501329, 2010.
- [31] L. P. Yaroslavsky. Digital picture processing - an introduction. *Springer Verlag*, 1985.
- [32] K. Zhang, W. Zuo, Y. Chen, D. Meng, and L. Zhang. Beyond a gaussian denoiser: Residual learning of deep cnn for image denoising. *IEEE Transactions on Image Processing*, 26(7):3142–3155, 2017.

## Appendices

In the following, based on the work in [28] we present a proof for Theorem 1 that shows Noise2Sim tends to be equivalent to Noise2Noise under realistic assumptions. Then, we report on the construction of datasets for evaluating Noise2Sim under ideal conditions, our expected results, as well as pilot data of extending Noise2Sim for removing structured noises.

### A. Proof of Theorem 1

Let  $s_i, s_i + n_i \in \mathbb{R}^{HW}$ , where  $H, W$  are the height and width of an image, respectively denote paired clean and noisy images, the Noise2Clean method trains a denoising network under the mean squared error (MSE) loss:

$$\theta_c = \arg \min_{\theta} \frac{1}{N_c} \sum_{i=1}^{N_c} \|f(s_i + n_i; \theta) - s_i\|_2^2, \quad (6)$$

where  $f : \mathbb{R}^{HW} \rightarrow \mathbb{R}^{HW}$  is the function represented by the denoising neural network,  $\theta$  is the vector of parameters to be trained, and  $N_c$  is the number of paired samples for Noise2Clean.

Noise2Noise generates two realizations of the same sample to train the denoising model:

$$\theta_n = \arg \min_{\theta} \frac{1}{N_n} \sum_{i=1}^{N_n} \|f(s_i + n_i; \theta) - (s_i + n'_i)\|_2^2, \quad (7)$$

where  $n_i, n'_i \in \mathbb{R}^n$  are two independent noises, and  $N_n$  is the number of paired samples in Noise2Noise. It has been proved in [28] that Noise2Noise will converge to Noise2Clean when the number of data is sufficiently large. They proved the following proposition:

**Proposition 1 ([28]).** *If conditional expectation  $E[n'_i | s_i + n_i] = 0$ ,  $\forall \theta$  and  $i$ , then  $\lim_{N_n \rightarrow \infty} \theta_n = \theta_c$ .*

Given a single noisy image only, Noise2Sim randomly constructs paired similar images for training a denoising network:

$$\theta_s = \arg \min_{\theta} \frac{1}{N_s} \sum_{i=1}^{N_s} \|f(s_i + n_i; \theta) - (s_i + \delta_i + n'_i)\|_2^2, \quad (8)$$

where  $s_i + \delta_i \in \mathbb{R}^{HW}$  is the constructed similar image,  $\delta_i \in \mathbb{R}^{HW}$  is the difference image between the clean signals embedded in paired similar images, and  $N_s$  is the number of constructed similar paired images for Noise2Sim. We argue that Noise2Sim is functionally equivalent to Noise2Noise by modeling the random variable  $\delta_i$  as a new type of noise. Furthermore, Noise2Sim is also equivalent to Noise2Clean, since Noise2Noise is equivalent to Noise2Clean. Suppose that the conditional expectation of the difference  $\delta_i$  is zero, we have the following theorem:

**Theorem 2.** *If conditional expectation  $E[n'_i | s_i + n_i] = 0$ , and  $E[\delta_i | s_i + n_i] = 0, \forall \theta$  and  $i$ , then  $\lim_{N_s \rightarrow \infty} \theta_s = \lim_{N_n \rightarrow \infty} \theta_n = \theta_c$ .*

*Proof.* Let  $y_i := f(s_i + n_i; \theta)$ , expanding the loss function in (8) and removing the terms that are irrelevant to  $\theta$  we have

$$\begin{aligned} & \arg \min_{\theta} \frac{1}{N_s} \sum_{i=1}^{N_s} \|y_i - (s_i + n'_i + \delta_i)\|_2^2 \\ &= \arg \min_{\theta} \frac{1}{N_s} \sum_{i=1}^{N_s} \|y_i - s_i\|_2^2 - \frac{1}{N_s} \sum_{i=1}^{N_s} 2n_i'^T y_i \\ & \quad - \frac{1}{N_s} \sum_{i=1}^{N_s} 2\delta_i^T y_i. \end{aligned} \quad (9)$$

According to the central limit theorem [?], the second and third terms respectively become

$$\begin{aligned} \lim_{N_s \rightarrow \infty} \frac{1}{N_s} \sum_{i=1}^{N_s} 2n_i'^T y_i &= 2E[n_i'^T y_i] \\ \lim_{N_s \rightarrow \infty} \frac{1}{N_s} \sum_{i=1}^{N_s} 2\delta_i^T y_i &= 2E[\delta_i^T y_i]. \end{aligned} \quad (10)$$

Because

$$\begin{aligned} E[n_i'^T y_i] &= E[E[n_i' | y_i]^T y_i] = E[E[n_i' | s_i + n_i]^T y_i] = 0 \\ E[\delta_i^T y_i] &= E[E[\delta_i | y_i]^T y_i] = E[E[\delta_i | s_i + n_i]^T y_i] = 0, \end{aligned} \quad (11)$$

where the second equivalence in the above two equations is due to the fact that  $y_i = f(s_i + n_i; \theta)$  is deterministic.

Then, the following equations hold true:

$$\begin{aligned} \lim_{N_s \rightarrow \infty} \frac{1}{N_s} \sum_{i=1}^{N_s} 2\mathbf{n}'_i{}^T \mathbf{y}_i &= 0 \\ \lim_{N_s \rightarrow \infty} \frac{1}{N_s} \sum_{i=1}^{N_s} 2\delta_i^T \mathbf{y}_i &= 0. \end{aligned} \quad (12)$$

As a result, as  $N_s \rightarrow \infty$ ,

$$\begin{aligned} \arg \min_{\theta} \frac{1}{N_s} \sum_{i=1}^{N_s} \|\mathbf{y}_i - (\mathbf{s}_i + \mathbf{n}'_i + \delta_i)\|_2^2 \\ = \arg \min_{\theta} \frac{1}{N_n} \sum_{i=1}^{N_n} \|\mathbf{y}_i - (\mathbf{s}_i + \mathbf{n}_{i2})\|_2^2 \\ = \arg \min_{\theta} \frac{1}{N_c} \sum_{i=1}^{N_c} \|\mathbf{y}_i - \mathbf{s}_i\|_2^2. \end{aligned} \quad (13)$$

Therefore,  $\lim_{N_s \rightarrow \infty} \theta_s = \lim_{N_n \rightarrow \infty} \theta_n = \theta_c$   $\square$

In practice, although  $E[\delta_i | \mathbf{x}_i + \mathbf{n}_i] = 0$  cannot be totally ensured, it is a realistic approximation, as demonstrated in Subsection 4.3.1. Thus, Noise2Sim can be regarded as a well-justified surrogate of Noise2Noise, and is applicable to noisy images individually.

In our implementation, we use two randomly reconstructed images, which are  $\mathbf{s}_i + \delta'_i + \mathbf{n}_i$  and  $\mathbf{s}_i + \delta_i + \mathbf{n}'_i$ , to train a denoising network, instead of using  $\mathbf{s}_i + \mathbf{n}_i$  and  $\mathbf{s}_i + \delta_i + \mathbf{n}'_i$ . Theoretically, they are equivalent as both of them are paired similar images. More specifically, Let  $\hat{\mathbf{s}}_i = \mathbf{s}_i + \delta'_i$ , then the randomly reconstructed pairs can be rewritten as  $\hat{\mathbf{s}}_i + \mathbf{n}_i$  and  $\hat{\mathbf{s}}_i + \delta''_i + \mathbf{n}'_i$ , where  $\delta''_i = \delta_i - \delta'$ . We can easily verify that  $E[\mathbf{n}'_i | \hat{\mathbf{s}}_i + \mathbf{n}_i] = \mathbf{0}$  and  $E[\delta''_i | \hat{\mathbf{s}}_i + \mathbf{n}_i] = \mathbf{0}$ , and Theorem 1 is still true. The advantage of such an implementation is that the capacity of possible image pairs can be significantly increased from  $(k+1)^{HW}$  to  $(k+1)^{2HW}$ , leading to a better performance as demonstrated in Subsection 4.3.2.

## B. Construction of a Dataset for an Ideal Experiment

To test the denoising performance of Noise2Sim under the ideal condition that the similarity error  $\delta_i = 0$ ,  $\forall i$ , we constructed a set of piecewise constant images of random rectangles. Specifically, let a  $128 \times 128$  image with zero values (8 bits per pixel) be the background, then certain random number ( $[0, 6]$ ) of randomly-sized rectangles were superimposed at random positions, each of which was filled with a random value. Finally, every synthesized image was normalized to  $[0, 255]$ . In this experiment, the training and testing datasets contain 2000 images respectively, and the Gaussian noise of *Std* of 25 was added to each image. Our results on these images verify the correctness of Noise2Sim.

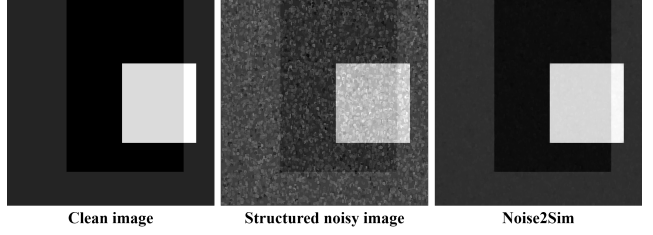


Figure 7. Results of denoising an image with structured noise.

## C. Pilot Results on Reduction of Structured Noises

The common limitation of both Noise2Sim and Noise2Void methods is that they cannot remove structured noise, since noise values for different pixels are not independent, violating the conditional independence assumption. Without additional prior knowledge, it is difficult to distinguish structured noises from real structures. Therefore, the Structured Noise2Void method [3] was developed under the assumption that the shape of noise is known, based on which the corresponding mask of the same shape is utilized during training.

Here we show the possibilities of extending Noise2Sim to process complex structured noises. Particularly, we show that if the segmentation mask of similar image regions are known, Noise2Sim can remove the complex structured noises. To satisfy this assumption, we constructed a set of piece-wise constant images similar to those in Section B, the differences are that the eclipses were replaced by rectangles in a  $512 \times 512$  background image, and the structured noises were added. Specifically, the English alphabet letters were randomly selected as structured noise, as shown in Figure 7. As structured noises are not pixel-wise independent, the construction of training samples were extended from pixel-level to patch-level. That is, we first extracted two sets of  $64 \times 64$  patches by sliding a window with a step of 32 on the noisy image and the clean image (equivalent to the segmentation mask), respectively. Then, for each noisy patch, a set of 8 similar patches were found, where the similarity between patches was evaluated on the corresponding clean patches using the Euclidean distance. During training, the network was optimized by learning to map between similar patches that were randomly selected and paired. The results in Figure 7 show that this extension of Noise2Sim under the ideal condition can remove the complex structured noises.